

# Experiments and nonlocal continuum modeling of the size-dependent fracture in elastomers<sup>[\[1,2\]](#)</sup>

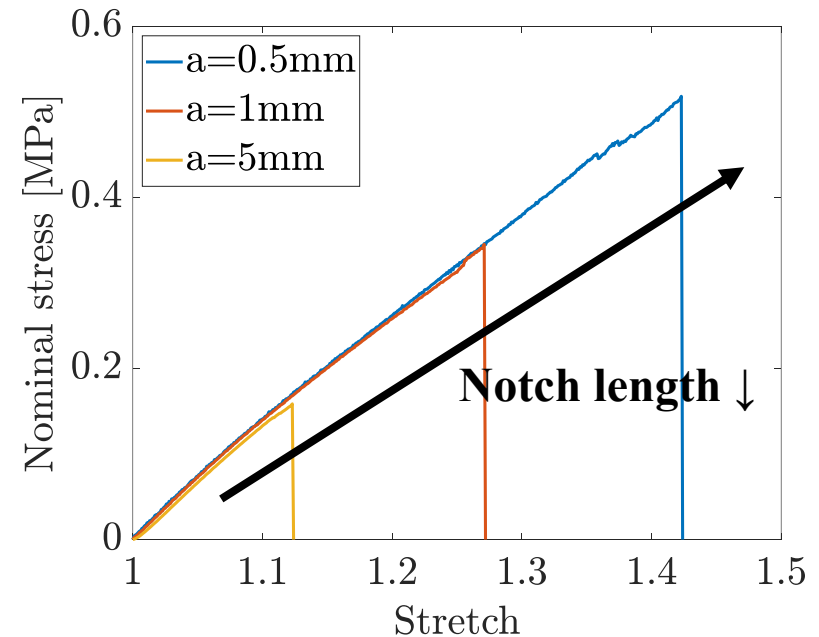
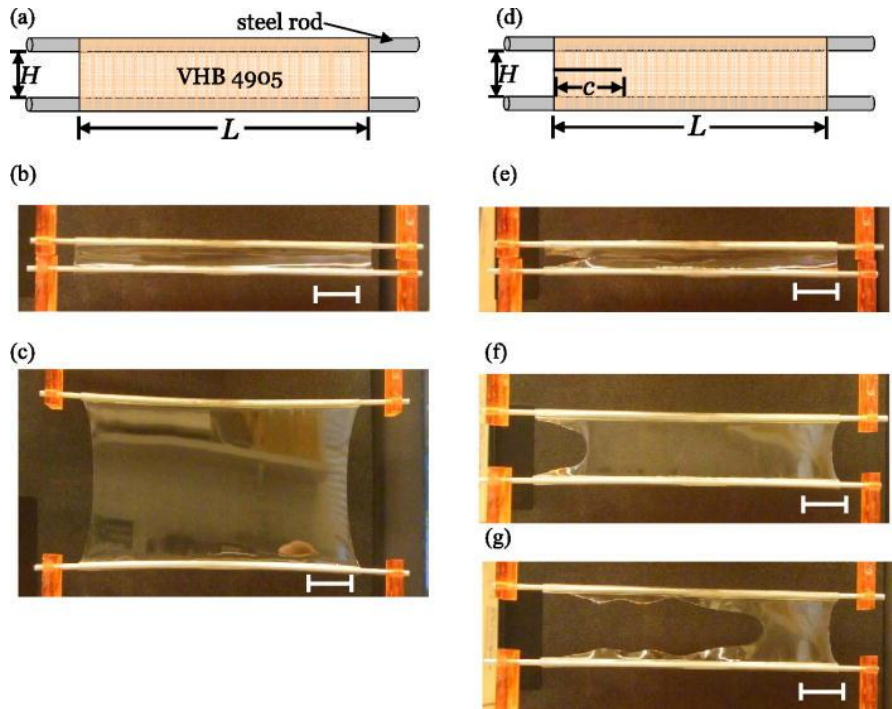
Jeongun Lee, Jaehee Lee and Hansohl Cho\*

Korea Advanced Institute of Science and Technology

\* hansohl@kaist.ac.kr

# Fracture in elastomers

- Extreme, nonlinear deformation  $\rightarrow$  fracture
- Influenced by the size of flaws; **the size-dependent fracture**<sup>[1,3]</sup>
  - Rupture stretch increases as the specimen size decreases

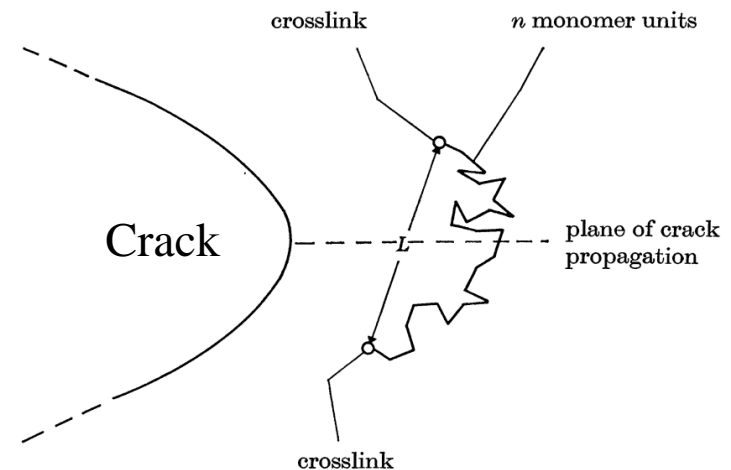
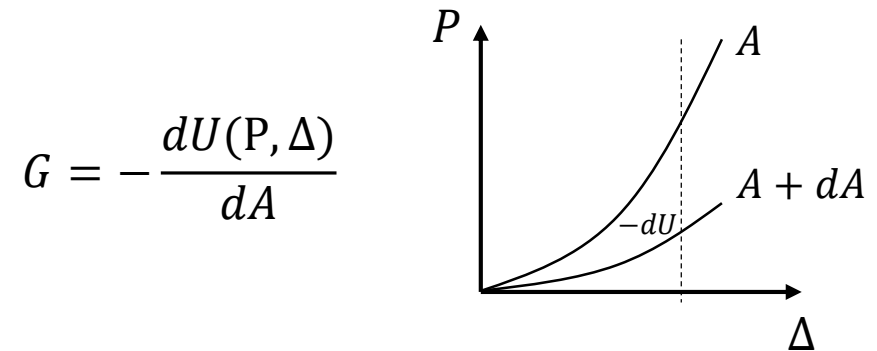


a) The presence of flaws impacts the fracture behavior<sup>[4]</sup>

b) Size-dependent fracture in polydimethylsiloxane (PDMS) specimens

# Fracture in elastomers

- Occurs when ...
  - Macroscopically, **G reaches  $\Gamma$** 
    - Griffith theory<sup>[5,6]</sup>
    - G: Energy release rate
    - $\Gamma$ : Fracture energy
  - Microscopically,  **$\epsilon_R$  reaches  $\epsilon_R^f$** 
    - Lake-Thomas theory<sup>[7-9]</sup>
    - $\epsilon_R$ : Internal energy
    - $\epsilon_R^f$ : critical internal energy;  
bond dissociation energy
- These approaches are compatible (Lake and Thomas <sup>[7]</sup>)



# Objectives

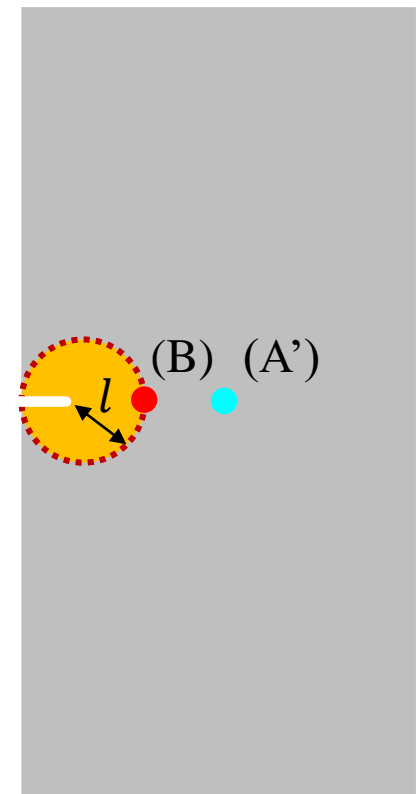
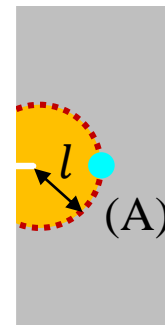
- Predicting the **size-dependent fracture** in elastomers<sup>[1]</sup>
  - Experiments and numerical simulations<sup>[2]</sup> were carried out
- **Internal energy-driven** fracture criterion; inspired by the Lake-Thomas model<sup>[7-9]</sup>
- Using the **phase-field model** rooted in the gradient-damage theory<sup>[2,9-13]</sup>
  - Mesh-insensitive crack propagation process
  - The internal energy-driven fracture criterion
  - Thermodynamics of the damage and fracture

# Size-dependent fracture & Fracture process zone

- Fracture process zone
  - Where the polymer chains rupture = Where the dissipation mainly occurs
- Stress at point (B) is larger than those at (A) and (A')
  - $\sigma_A = \sigma_{A'} < \sigma_B$
- → Free energy at point (B) is larger than those at (A) and (A')
  - $\psi_A = \psi_{A'} < \psi_B$
- →  $\psi_B$  reaches the critical energy earlier than  $\psi_A$
- → **The larger specimen ruptures earlier**

The size of fracture process zone<sup>[1,3,14,15]</sup>:

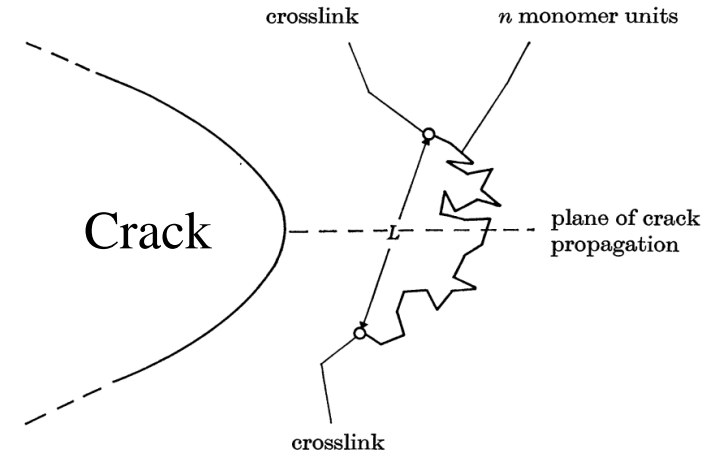
$$l = \frac{\Gamma}{W^*} = \frac{\text{Fracture energy}}{\text{Critical deformation energy}}$$



# Nonlocal continuum modeling

- 1. The damage  $d \in [0,1]$ 
  - $d=0$ : intact
  - $d=1$ : fully damaged
- Internal energy-driven** fracture criterion
  - Inspired by the Lake-Thomas model<sup>[5]</sup>
  - Fracture = **Scission of polymer chains**
- Governing equations<sup>[9]</sup>
  - Macroforce balance  $\text{Div } \mathbf{T}_R = 0$
  - Microforce balance  $\zeta \dot{d} = 2(1 - d)\mathcal{H}_R - \hat{\varepsilon}_R^f (d - l'^2 \Delta d)$

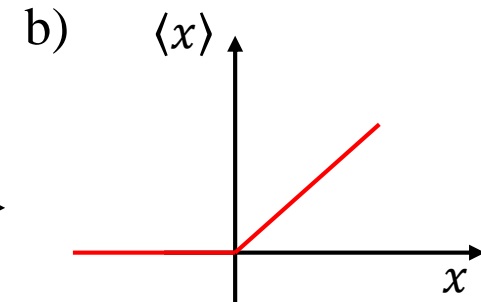
a)<sup>[7]</sup>



History function;  
the fracture criterion

$$\mathcal{H}_R = \left\langle \varepsilon_R^0 - \varepsilon_R^f / 2 \right\rangle, \quad \text{where } \langle x \rangle = \begin{cases} x & \text{if } x > 0 \\ 0 & \text{if } x \leq 0 \end{cases}$$

Internal energy



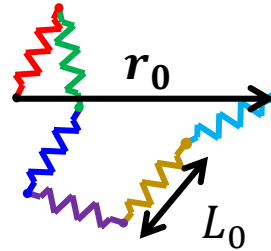
# Nonlocal continuum modeling

- **Internal energy** should be considered → **Bond stretch**<sup>[8,9]</sup>

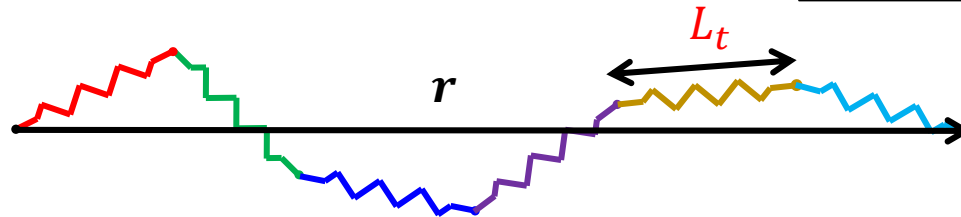
- Deformation = Chain configuration change + stretching of molecular bonds

$$\psi_R = \underbrace{(1-d)^2 \left[ \frac{1}{2} N n E_b (\lambda_b - 1)^2 + \frac{1}{2} K (J - 1)^2 \right]}_{(1-d)^2 \varepsilon_R^0; \text{ Damage acts on the internal energy only}} + \underbrace{N k_b \theta n \left[ \frac{\bar{\lambda} \lambda_b^{-1}}{\sqrt{n}} \beta + \ln \left( \frac{\beta}{\sinh \beta} \right) \right]}_{-\theta \eta_R; \text{ Entropic energy}} + \underbrace{\frac{1}{2} \varepsilon_R^f l^2 |\nabla d|^2}_{\text{Nonlocal energy}^{[9]}}$$

a) Reference configuration



a) Deformed configuration



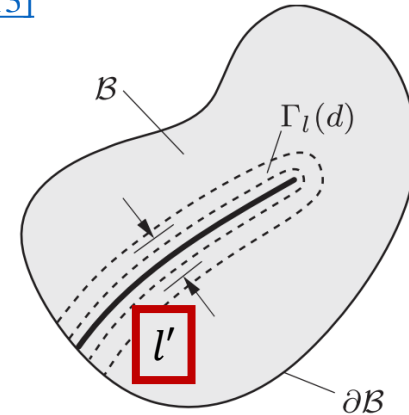
$$\begin{aligned} \bar{\lambda} &= \frac{|r|}{|r_0|} \\ \lambda_b &= \frac{L_t}{L_0} \\ \mathcal{L}(x) &= \coth x - \frac{1}{x} \\ \beta &= \mathcal{L}^{-1} \left( \frac{\bar{\lambda} \lambda_b^{-1}}{\sqrt{n}} \right) \end{aligned}$$

# Nonlocal continuum modeling

- 2. Phase-field model rooted in the gradient-damage theory<sup>[9-13]</sup>
  - “Diffusive damage zone”

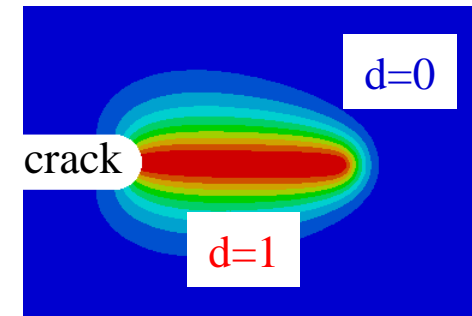
- Microforce balance  $\zeta \dot{d} = 2(1 - d)\mathcal{H}_R - \hat{\varepsilon}_R^f(d - \boxed{l'^2 \Delta d})$   
 History function;  
 the fracture criterion

a)<sup>[13]</sup>



- The **intrinsic length scale  $l'$**   $\rightarrow$  the size of diffusive damage zone
  - A numerical parameter; ambiguous physical meaning

b)



Crack propagation;  
at reference configuration



# Nonlocal continuum modeling

- Assumption<sup>[1]</sup>: Diffusive damage zone = Fracture process zone
  - Regions of the damage evolution and the dissipation

- The size of fracture process zone

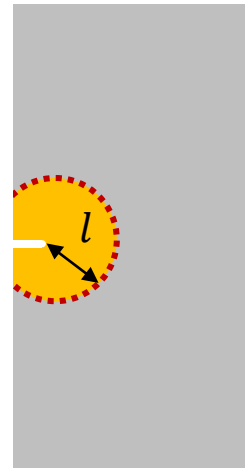
$$= \frac{\Gamma}{W^*} = \frac{\text{Fracture energy}}{\text{Critical deformation energy}} \rightarrow \text{Intrinsic length scale}$$

→ Identify the intrinsic length scale  $l$  **from experiments**

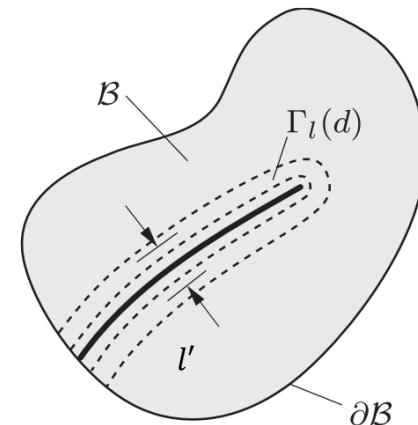
→ Apply to the phase field model

→ Predict the **size-dependent fracture** by numerical simulations<sup>[1]</sup>

a) Fracture process zone

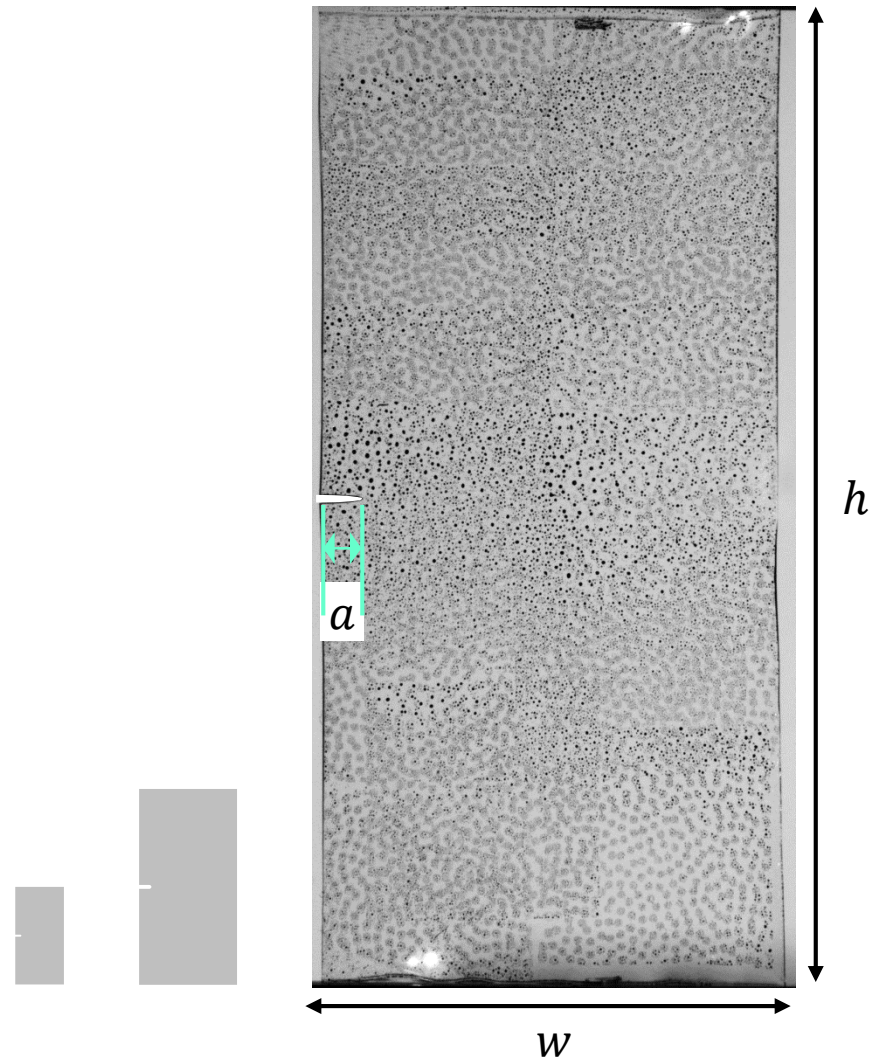


b)<sup>[13]</sup> Diffusive damage zone



# Experimental procedures<sup>[1]</sup>

- Geometries
  - $a = \{0.5, 1, 5\}$  mm
  - $w = 10a$ ,  $h = 20a$ , specimen thickness: 0.5mm
    - $w = \{5, 10, 50\}$  mm
    - $h = \{10, 20, 100\}$  mm
- Materials
  - PDMS
  - TangoPlus (3D-printed elastomer)
- Strain rate  $0.01 \text{ s}^{-1}$ , temperature  $\sim 21^\circ\text{C}$
- Digital image correlation (DIC) analysis
  - Strain fields from experiments



# The intrinsic length scale $l$

- $l = \frac{\Gamma}{W^*} \rightarrow$  **Experimentally identified intrinsic length scale**<sup>[1]</sup>
- $\Gamma$ : Fracture energy
  - from **notched** specimens
- $W^*$ : Critical deformation energy
  - from **unnotched** specimens

## PDMS

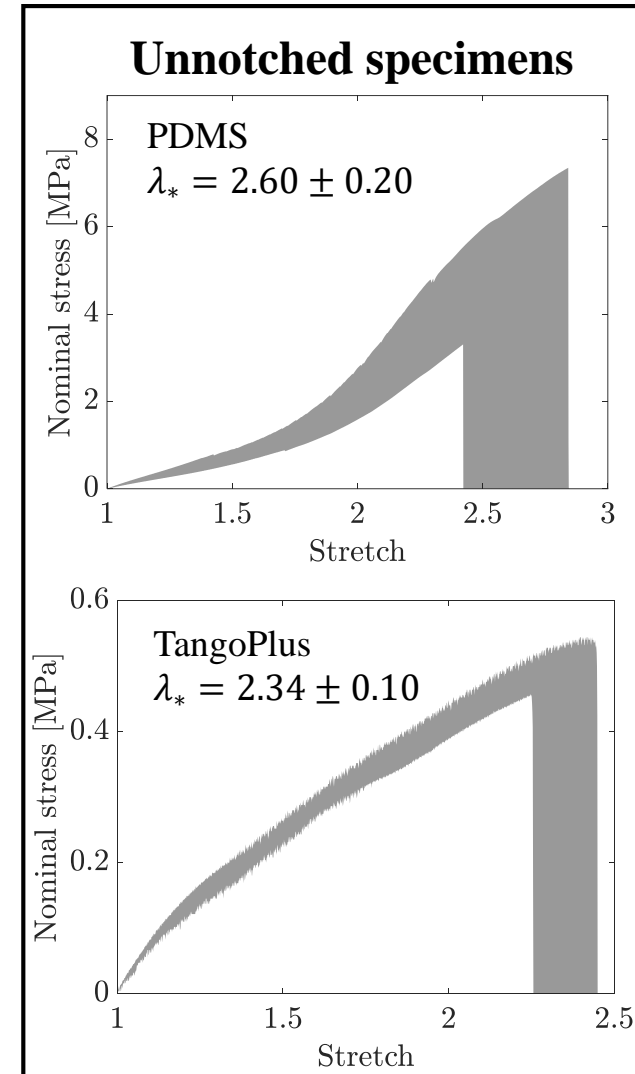
$$\Gamma \approx 0.25 \text{ mJ/mm}^2, W^* \approx 2.7 \text{ mJ/mm}^3$$

$$\rightarrow l \approx 0.08 \text{ mm}$$

## TangoPlus

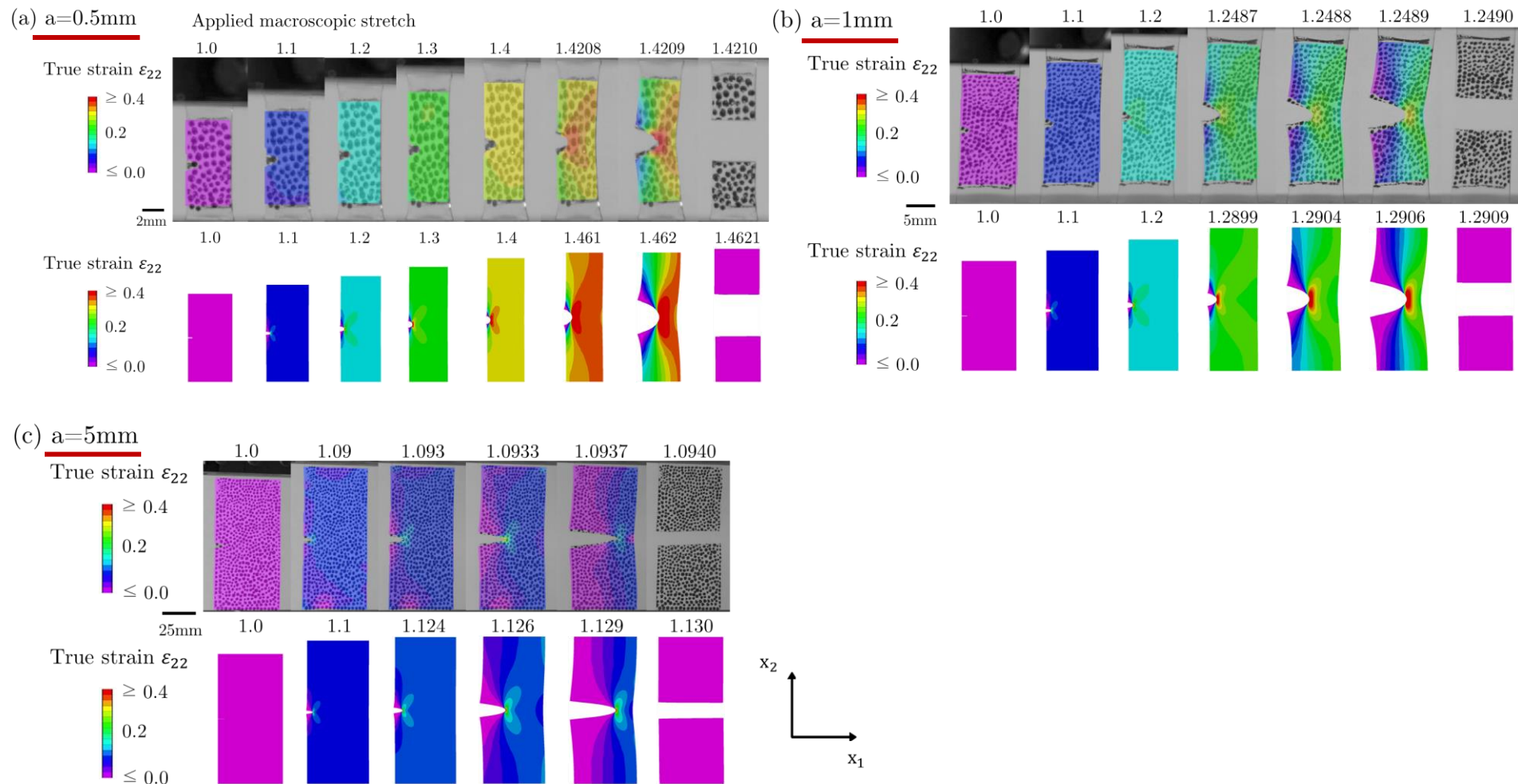
$$\Gamma = 0.5 \text{ mJ/mm}^2, W^* \approx 0.45 \text{ mJ/mm}^3$$

$$\rightarrow l \approx 1 \text{ mm}$$



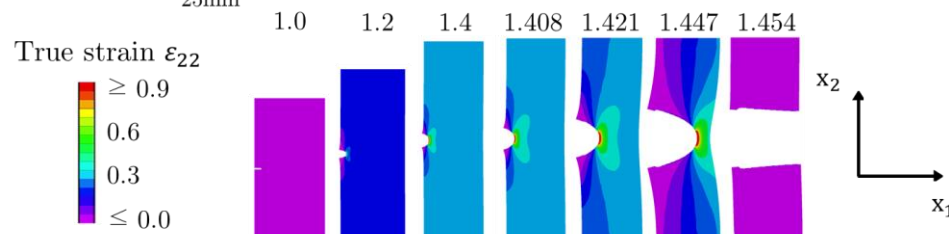
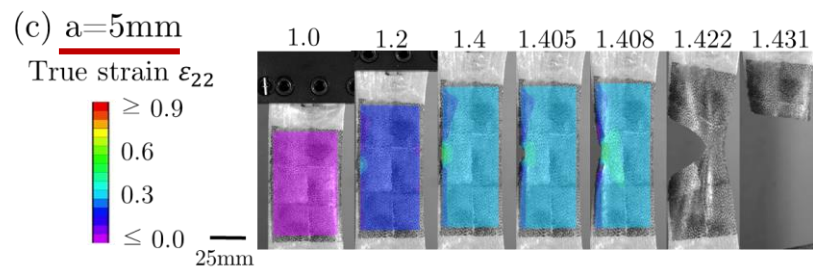
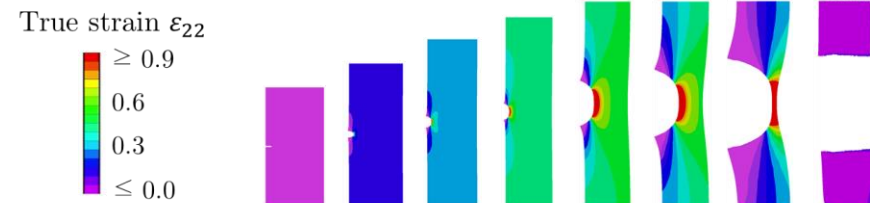
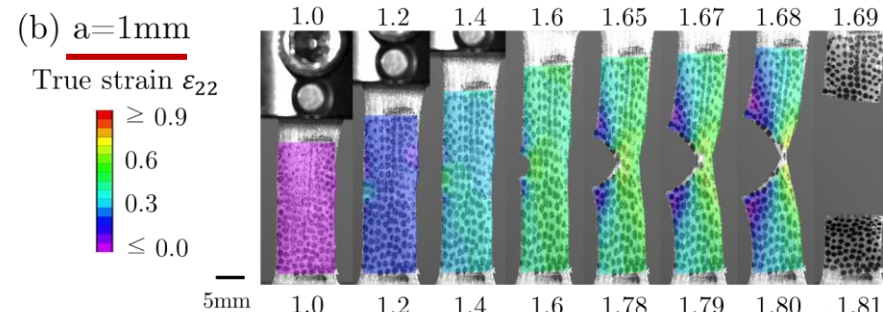
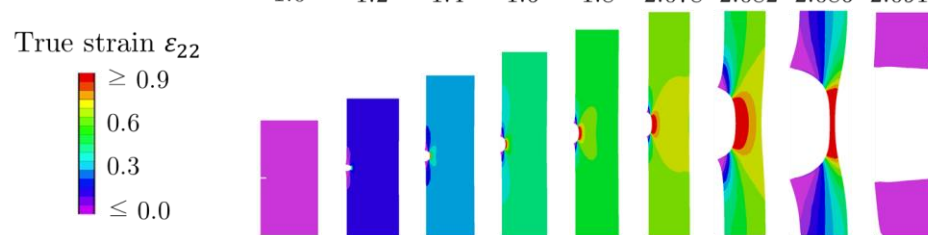
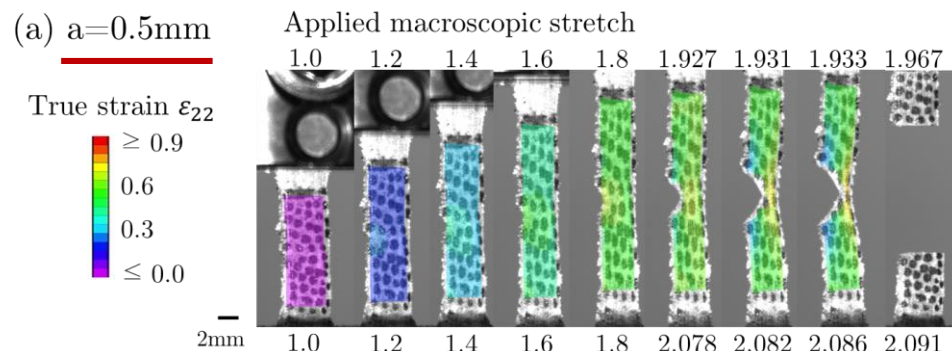
# Results: Experiment vs. Numerical simulation<sup>[1]</sup>

- Strain fields in **PDMS** specimens ( $l = 0.08mm$ )
  - Larger specimen ruptures earlier



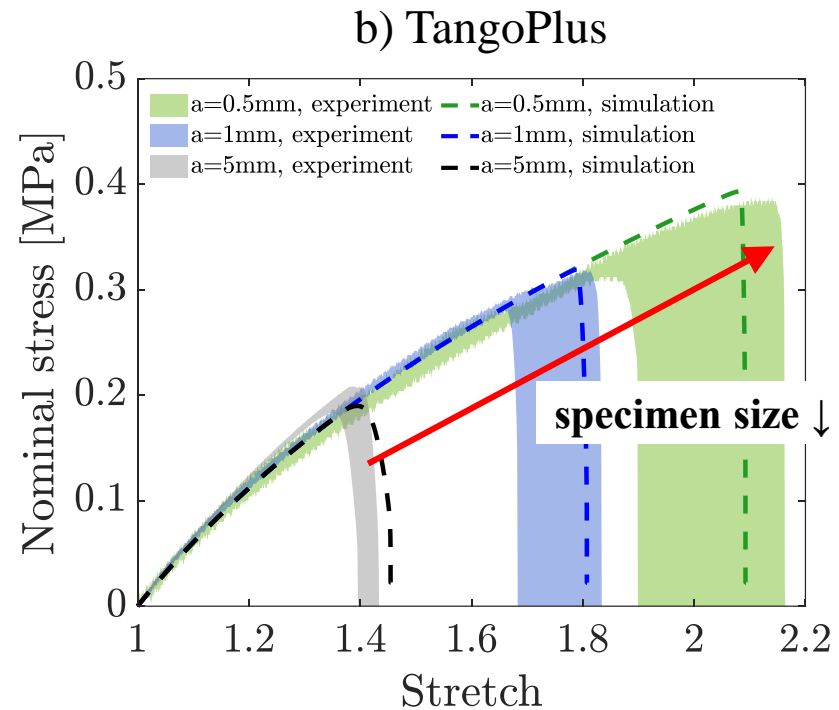
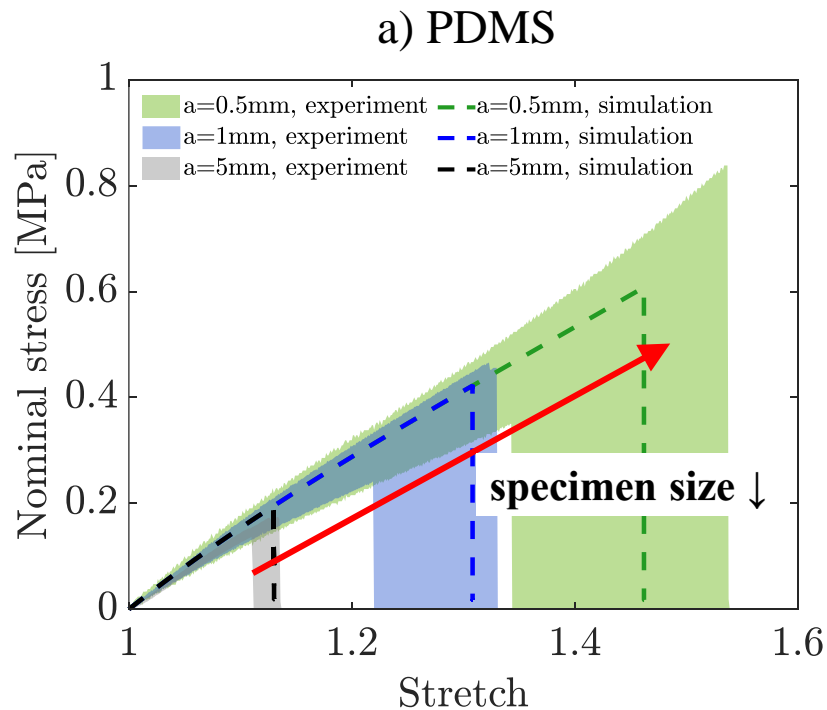
# Results: Experiment vs. Numerical simulation<sup>[1]</sup>

- Strain fields in **TangoPlus** specimens ( $l = 1mm$ )
  - Larger specimen ruptures earlier



# Results: Experiment vs. Numerical simulation<sup>[1]</sup>

- Notch lengths  $a = \{0.5, 1, 5\}$  mm
- Geometric similarity → **Identical initial stress-stretch response**
- Smaller notch length → Higher rupture stretch





# Notch-length sensitivity<sup>[1]</sup>

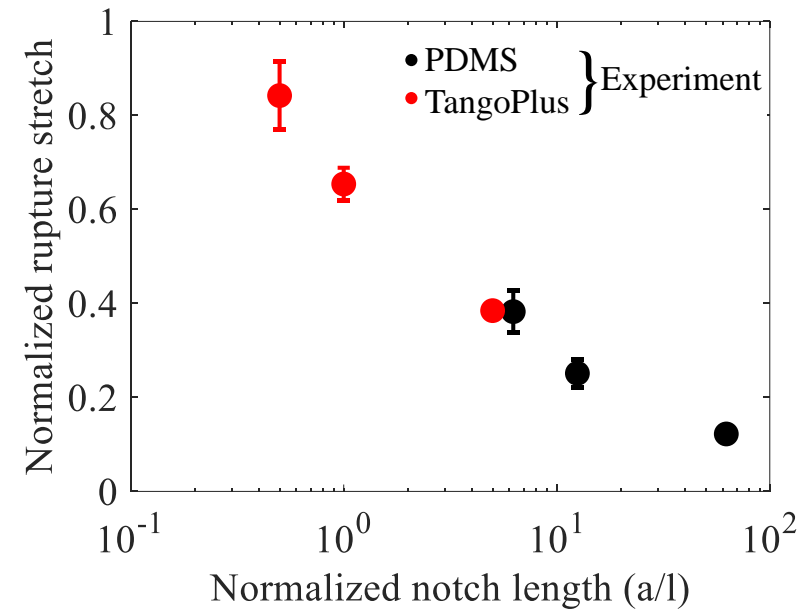
- PDMS vs. TangoPlus; same specimen sizes
  - PDMS:  $l = 0.08\text{mm}$
  - TangoPlus:  $l = 1\text{mm}$

More than 10 times

- Normalized rupture stretch

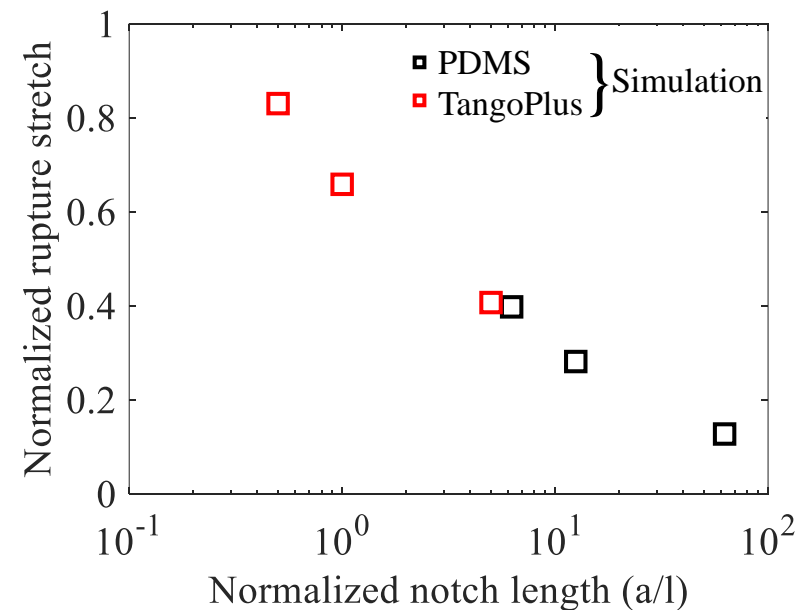
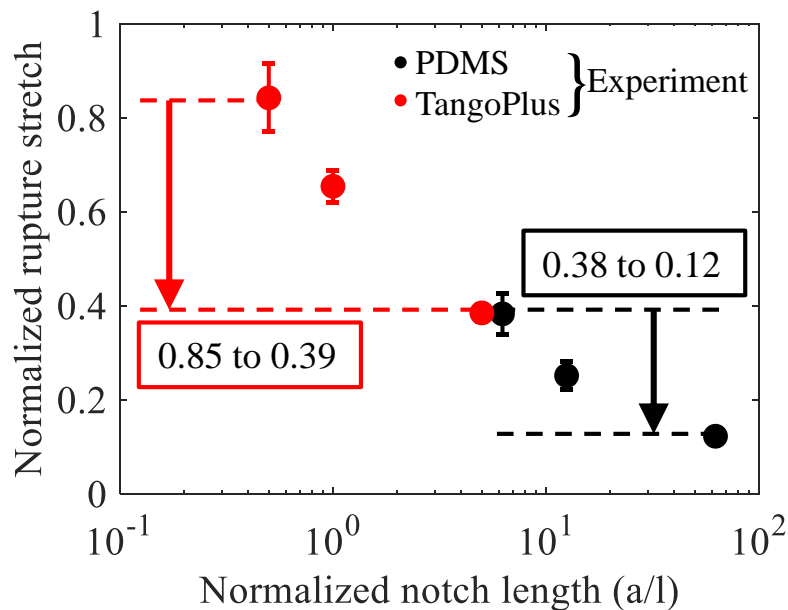
$$= \frac{\text{Rupture stretch of notched specimens}}{\text{Rupture stretch of unnotched specimens}}$$

- Normalized notch length =  $\frac{\text{Notch length (a)}}{\text{Intrinsic length scale (l)}}$



# Notch-length sensitivity<sup>[1]</sup>

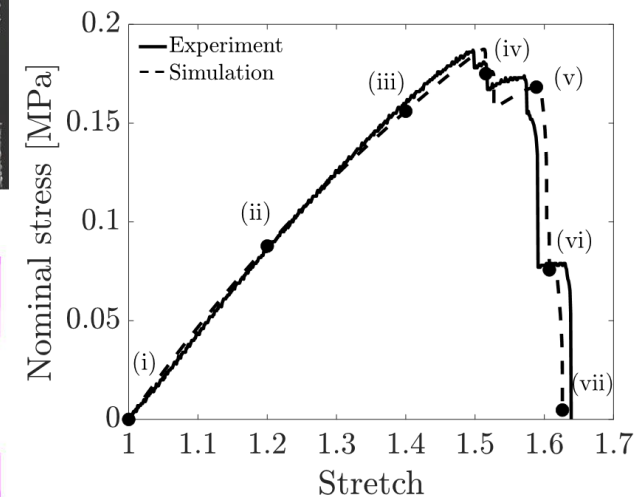
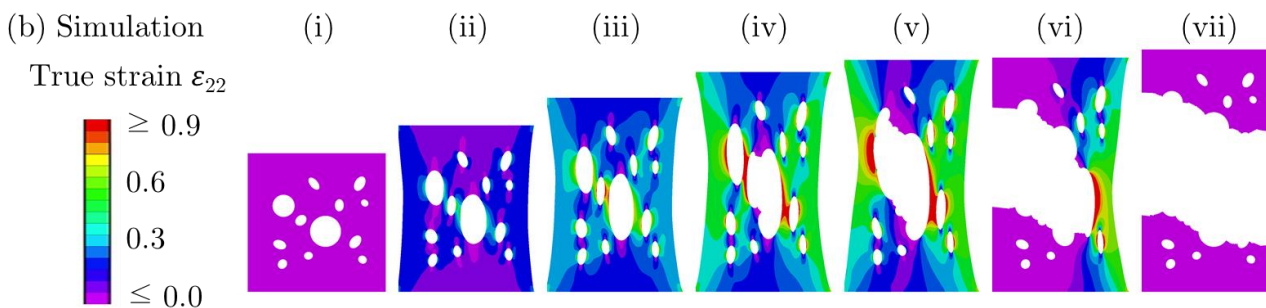
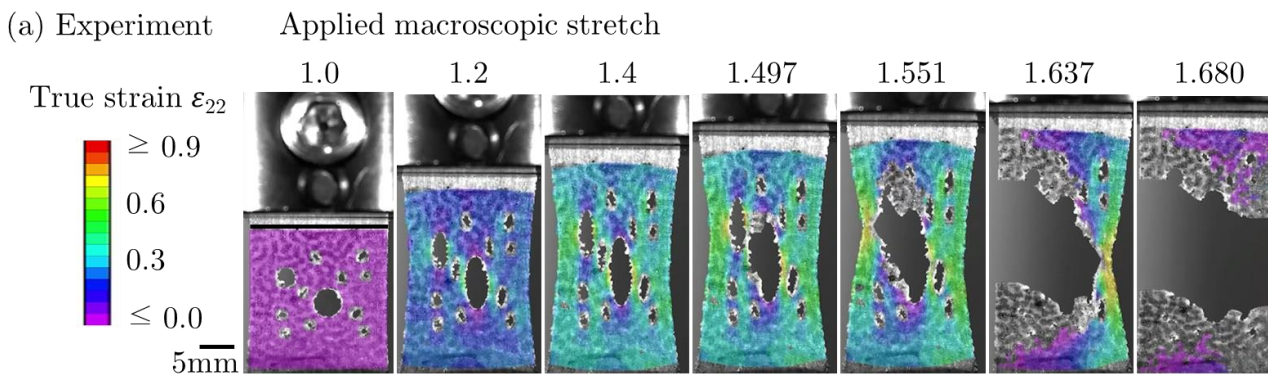
- PDMS vs. TangoPlus; same specimen sizes
  - PDMS:  $l = 0.08\text{mm}$
  - TangoPlus:  $l = 1\text{mm}$
 ) **More than 10 times**
- $a/l$ : 0.5~5 (TangoPlus;  $l = 1\text{mm}$ ) → Highly notch length-sensitive
- $a/l$ : 5~50 (PDMS;  $l = 0.08\text{mm}$ ) → Less notch length-sensitive





# Randomly perforated specimen (TangoPlus)<sup>[1]</sup>

- Nicely predicted the response **without modification of parameters**
  - Progressive fracture of ligaments

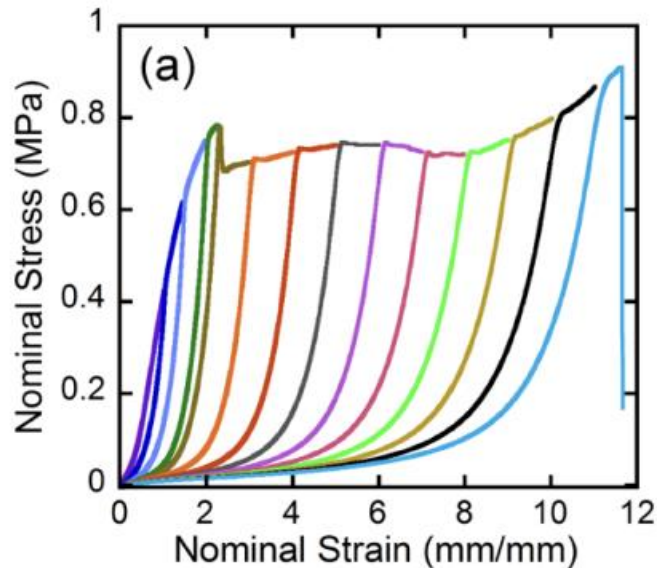


# Conclusion

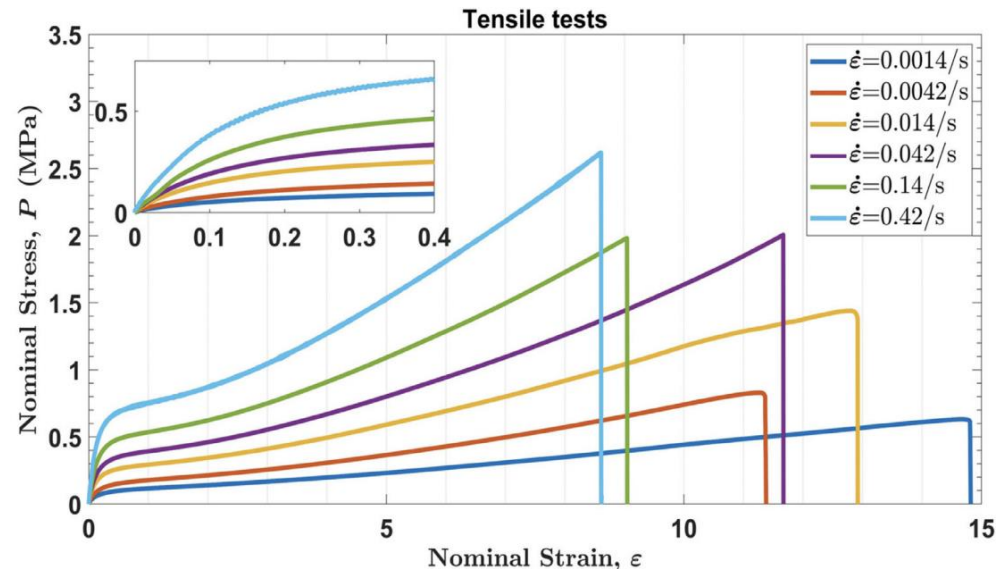
- **Size-dependent fracture** is clearly observed in experiments<sup>[1]</sup>
  - Rupture stretch increases as the notch length decreases
  - Size-dependence increases as the notch-root radius decreases
- **The intrinsic length scale** is central to account for the size-dependent behavior<sup>[1]</sup>
  - The intrinsic length scale  $l$  defines the size of diffusive damage zone / fracture process zone
  - The intrinsic length scales were identified from experiments
  - Normalized notch length ( $a/l$ ) determines the size-dependence
- **Nonlocal continuum model**<sup>[2,9]</sup> nicely predicted the fracture in elastomers<sup>[1]</sup>
  - Nonlocal continuum model utilizes experimentally identified intrinsic length scales
  - The model captures the size-dependent fracture in elastomers
  - The model is capable of predicting the fracture of complex geometries

# Future work

- Fracture involving non-trivial dissipation
  - Mullins effect [\[16-20\]](#)
    - Is the fracture behavior influenced by the rate-independent dissipation (e.g., the Mullins effect) ?
  - Viscous dissipation [\[16-19,21\]](#)
    - How to describe complicated deformation and fracture behaviors in polymers?



a) Fracture in double-network elastomers; the Mullins effect and fracture occur [\[20\]](#)



b) Rate-dependent deformation and fracture behaviors in a hydrogel (polyampholyte gel) [\[21\]](#)

# References

- [1] Lee, J., Lee, J., Yun, S., Kim, S., Lee, H., Chester, S. A., & Cho, H. (2024). Size-dependent fracture in elastomers: Experiments and continuum modeling. *Physical Review Materials*, 8(11), 115602.
- [2] Lee, J., Lee, S., Chester, S. A., & Cho, H. (2023). Finite element implementation of a gradient-damage theory for fracture in elastomeric materials. *International Journal of Solids and Structures*, 279, 112309.
- [3] Chen, C., Wang, Z., & Suo, Z. (2017). Flaw sensitivity of highly stretchable materials. *Extreme Mechanics Letters*, 10, 50-57.
- [4] Pharr, M., Sun, J. Y., & Suo, Z. (2012). Rupture of a highly stretchable acrylic dielectric elastomer. *Journal of Applied Physics*, 111(10).
- [5] Griffith, A. A. (1921). VI. The phenomena of rupture and flow in solids. *Philosophical transactions of the royal society of london. Series A, containing papers of a mathematical or physical character*, 221(582-593), 163-198.
- [6] Rivlin, R. S., & Thomas, A. G. (1953). Rupture of rubber. I. Characteristic energy for tearing. *Journal of polymer science*, 10(3), 291-318.
- [7] Lake, G. J., & Thomas, A. G. (1967). The strength of highly elastic materials. *Proceedings of the Royal Society of London. Series A. Mathematical and Physical Sciences*, 300(1460), 108-119.
- [8] Mao, Y., Talamini, B., & Anand, L. (2017). Rupture of polymers by chain scission. *Extreme Mechanics Letters*, 13, 17-24.
- [9] Talamini, B., Mao, Y., & Anand, L. (2018). Progressive damage and rupture in polymers. *Journal of the Mechanics and Physics of Solids*, 111, 434-457.

# References

- [10] Peerlings, R. H., de Borst, R., Brekelmans, W. M., & de Vree, J. (1996). Gradient enhanced damage for quasi-brittle materials. [\*International Journal for numerical methods in engineering\*, 39\(19\), 3391-3403.](#)
- [11] De Borst, R., Pamin, J., & Geers, M. G. (1999). On coupled gradient-dependent plasticity and damage theories with a view to localization analysis. [\*European Journal of Mechanics-A/Solids\*, 18\(6\), 939-962.](#)
- [12] Francfort, G. A., & Marigo, J. J. (1998). Revisiting brittle fracture as an energy minimization problem. [\*Journal of the Mechanics and Physics of Solids\*, 46\(8\), 1319-1342.](#)
- [13] Miehe, C., Welschinger, F., & Hofacker, M. (2010). Thermodynamically consistent phase-field models of fracture: Variational principles and multi-field FE implementations. [\*International journal for numerical methods in engineering\*, 83\(10\), 1273-1311.](#)
- [14] Bažant, Z. P. (1997). Scaling of quasibrittle fracture: asymptotic analysis. [\*International Journal of Fracture\*, 83, 19-40.](#)
- [15] Yang, C., Yin, T., & Suo, Z. (2019). Polyacrylamide hydrogels. I. Network imperfection. [\*Journal of the Mechanics and Physics of Solids\*, 131, 43-55.](#)
- [16] Cho, H., Rinaldi, R. G., & Boyce, M. C. (2013). Constitutive modeling of the rate-dependent resilient and dissipative large deformation behavior of a segmented copolymer polyurea. [\*Soft Matter\*, 9\(27\), 6319-6330.](#)
- [17] Cho, H., Mayer, S., Pöselt, E., Susoff, M., in't Veld, P. J., Rutledge, G. C., & Boyce, M. C. (2017). Deformation mechanisms of thermoplastic elastomers: Stress-strain behavior and constitutive modeling. [\*Polymer\*, 128, 87-99.](#)
- [18] Lee, J., Veyssset, D., Hsieh, A. J., Rutledge, G. C., & Cho, H. (2023). A polyurethane-urea elastomer at low to extreme strain rates. [\*International Journal of Solids and Structures\*, 280, 112360.](#)

# References

- [19] Cho, H., Lee, J., Moon, J., Pösel, E., Rutledge, G. C., & Boyce, M. C. (2024). Large strain micromechanics of thermoplastic elastomers with random microstructures. [\*Journal of the Mechanics and Physics of Solids\*, 187, 105615.](#)
- [20] Nakajima, T., Fukuda, Y., Kurokawa, T., Sakai, T., Chung, U. I., & Gong, J. P. (2013). Synthesis and fracture process analysis of double network hydrogels with a well-defined first network. [\*ACS Macro Letters\*, 2\(6\), 518-521.](#)
- [21] Venkata, S. P., Cui, K., Guo, J., Zehnder, A. T., Gong, J. P., & Hui, C. Y. (2021). Constitutive modeling of bond breaking and healing kinetics of physical Polyampholyte (PA) gel. [\*Extreme Mechanics Letters\*, 43, 101184.](#)